Supplementary Information for

Treatment with an Antigen-Specific Dual Microparticle System Reverses Advanced Multiple Sclerosis in Mice

Alexander J Kwiatkowski[1], Eric Y Helm[2], Joshua M Stewart[1], Theodore T Drashansky[2], Jonathan J Cho[2], Dorina Avram[2,3*] and Benjamin G Keselowsky[1,4*]
[1] J. Crayton Pruitt Family Department of Biomedical Engineering, University of Florida, Gainesville, FL 32611, USA
day [2]epartment of Anatomy and Cell Biology, College of Medicine, University of Florida, Gainesville, FL 32610, USA
[3] H. Lee Moffitt Cancer Center & Research Institute, Tampa, FL 33612
[4] Department of Pathology, Immunology and Laboratory Medicine, College of Medicine, University of Florida, Gainesville FL 32610, USA.

*Co-corresponding authors: Benjamin G. Keselowsky; Dorina Avram

Email: Bkeselowsky@bme.ufl.edu, Dorina.Avram.moffitt.org

This PDF file includes:

Extended Methods

Microparticle Formulation:

50:50 PLGA (MW ~ 65,000 g/mol) (Purac) was used for formulation of all MPs. 500 mg of PLGA was dissolved in 2.5 mL methylene chloride for non-phagocysotable MPs or 10 mL for phagocytosable MPs and placed on a shaker for 20 minutes at room temperature. 50 µg VD3 (Cayman Chemical) was dissolved in 1mL of methanol then added to the PLGA dissolved in methylene chloride. This solution was added to 50 mL of polyvinyl alcohol (PVA) and used a tissue homogenizer at 35,000 rpm for 120 seconds to create the single emulsion. For water soluble MOG and OVA (Mimotopes), factors were dissolved in sterile PBS and added to 10mL methylene chloride PLGA solution and homogenized at 35, 000 rpm for 120 seconds to form the primary emulsion. This solution was added dropwise to 50 mL of 5% PVA and emulsified for 120 seconds at 35,000 rpm to form the secondary emulsion. GM-CSF and TGF-β were dissolved in sterile PBS and placed in a solution of 2.5 mL methylene chloride and PLGA. This solution was then vortexed at 3200 rpm for 120 seconds. 5 mL of 2.5% PVA was added to this solution dropwise and emulsified on a vortex for 120 seconds at 3200 rpm. All MPs were added to 100 mL of 1% PVA and stirred for 5 hours. Following stirring, MPs were centrifuged at 18,000 G for 10 minutes. The MPs were washed 3x in nanopure water and centrifuged at 18,000 G for 10 minutes after each wash. After washing, MPs were flash froze in liquid nitrogen and lyophilized for 48 hours. MPs were checked for endotoxin via chromo-lal and stored at -80 °C until use.

Microparticle Characterization:

Phagocytosable MPs were sized on the Malvern Zetasizer Ultra (Malvern Panalytical), while non-phagocytosable MPs were sized on the LS13320 (Beckman Coulter). Size is reported as mean volume percentage ± standard deviation. Encapsulation efficiency of MOG, OVA, TGF-β1 and GM-CSF MPs used CBQCA (ThermoFisher). Briefly MPs were dissolved in 0.1 M sodium borate in an amount such that a 10% encapsulation efficiency would be above the limit of detection for the assay. Following addition of sodium borate the samples were placed in a sonication bath for 20 minutes. CBQCA reagent and potassium cyanide were added to the samples according to manufacturer's protocol. One hour later a plate reader determined the fluorescence. Importantly, the standard curve used the factor of interest rather than the BSA provided in the kit. Quantification of VD3 MPs involved dissolving the PLGA then measuring VD3 via spectrophotometer. To evaluate release kinetics, MPs were placed in a microcentrifuge tube in amount such that 2% factor release could be detected. MPs were suspended in PBS and placed on a shaker at 37 °C. The MPs were spun down at 10,000 G and the supernatant was collected to be used in for evaluation of release. CBQCA was used for MOG, OVA, GM-CSF and TGF-β MPs, while spectrometry determined VD3 release. Samples were stored at -20 °C until the release was quantified.

Acquiring a single cell suspension from CNS:

Following euthanasia, perfusion through the right ventricle with 10 mL of ice-cold PBS cleared circulating cells from the CNS vasculature. A gentleMACS dissociator (Miltenyi Biotec) homogenized the tissue following the brain and spinal cord harvest. Collagenase A (0.33 mg/mL) digestion for 25 minutes shaking at 37

^{o}C followed by mechanical dissociation through a 70 μm filter removed excess CNS tissue. Following centrifugation at 380 G for five minutes, a 30% isotonic Percoll (GE Healthcare), underlaid with 70% isotonic Percoll and spun at 650 G for 25 minutes with no brake separated red blood cells, immune cells and myelin. The interphase between the 30-70% layers contained mononuclear cells, and these were stained for flow cytometry or prepared for single-cell RNA sequencing.

Histological Analysis

Using the Leica protocol, samples were dehydrated with ethanol starting with 90% and two rinses of 100% for 15 minutes each. Cleaning then used three xylene washes for 20, 20, and 45 minutes, respectively. Samples were exposed to paraffin wax for three changes of 30, 30, and 45 minutes, respectively. The spinal cord was embedded (Tissue-Tek) so that the L1 vertebrae was the first cross-section cut and ended at L6. The blocks were sectioned at 4 μm and dried overnight before staining. All staining sections were deparaffinized by the following: two five minute changes of xylenes, two three minute changes of 100% ethanol, one minute change of 95% ethanol, and a rinse in deionized water. H&E staining utilized a kit from Vector labs. Briefly, the protocol was 5 minutes in hematoxylin, two rinses of deionized water, bluing reagent for 15 seconds, rinsed in 100% ethanol, 3 minutes in Eosin Y, and three two minute rinses in 100% ethanol then coverslipped. For luxol fast blue staining, after deparaffinization, 0.1% LFB was added to the slides for two hours at 60 ^{0}C followed by a three minute change in 70% ethanol and a change in each deionized water, lithium carbonate, and distilled water. Counterstain used cresyl violet for 10 minutes followed by rinses in 95% ethanol and xylenes twice; then the slides were

coverslipped. Imaging at 5x and 20x magnification took place on a Zeiss Axio Inverted Microscope (Carl Zeiss).

Multiplex Immunofluorescence

Formalin-fixed and paraffin-embedded (FFPE) tissue samples were immunostained using the AKOAYA Biosciences OPAL TM 7-Color Automation IHC kit on the BOND RX autostainer (Leica Biosystems). The OPAL 7-color kit uses tyramide signal amplification (TSA)-conjugated to individual fluorophores to detect various targets within the fluorescent multiplex assay.

Sections were baked at 65 °C for three hours then transferred to the BOND RX (Leica Biosystems). All subsequent steps (ex., deparaffinization, antigen retrieval) were performed using an automated OPAL IHC procedure (AKOYA). OPAL staining of each antigen occurred as follows: heat induced epitope retrieval (HIER) was achieved with EDTA pH 9.0 buffer for 20 minutes at 95°C before the slides were blocked with AKOYA blocking buffer for 10 minutes. Then slides were incubated with primary antibody and one of the OPAL fluorophores during the final TSA step. Staining used the following antibodies, TMEM119 (Abcam, 28-3, HIER- EDTA pH 9.0, 1:100, dye 570), Ki67 (Abcam, SP6, HIER- Citrate pH 6.0, 1:300, dye 620), CD74 (LS Bio, Rb poly, HIER- EDTA pH 9.0, 1:600, dye 520), GFAP (Abcam, EPR1034Y, HIER- EDTA pH 9.0, 1:500, dye 540), CD4 (CST, D7D2Z, HIER- EDTA pH 9.0, 1:100, dye 650), and CD8 (CST, D4W2Z, HIER- EDTA pH 9.0, 1:100, dye 690). All slides were imaged with the Vectra®3 Automated Quantitative Pathology Imaging System. Individual antibody complexes were stripped after each round of antigen detection. After

the final stripping step, DAPI counterstain is applied to the multiplexed slide and is removed from BOND RX for coverslipping with ProLong Diamond Antifade Mountant (ThermoFisher Scientific).

Antibodies

Cells were stained with the following antibodies: CD11b (BV510, clone: M1/70), CD11c (BV711, clone: N418), F4/80 (PE, PE-Cy7, clone: BM8), MHCII (BV421, APC-ef780, clone: M5/114.15.2), TCR-β (ef450, clone: H57-597), Ly6c (Pacific Blue, clone:HK1.4), Ly6g (PE-Dazzle594, clone: 1A8), CD8α (BV605, SB600, clone: 53-6.7), CD86 (PE-Cy5, APC, clone: GL1), CD4 (BV785, SB780, clone: RM4-5), GR-1 (PE_Cy7, clone: RB6-8C5), CD19 (APC, clone: 1D3), CD45.2 (AF700, clone:104), B220 (BV650, clone: RA3-6B2). Tmem119 (af488, clone: V3RT1GOsz, 28-3), CD74 (AF647, clone: In1/CD74), CD3ε (BV650, clone: 145-2C11), Ki-67 (PE-Dazzle594, clone: 16a8), Foxp3 (PE-cf594, clone: MF23), Rorγt (APC, clone: AFKJS-9), tbet (BV421, clone: 4B10), IL-23R (BV421, clone: 12B2B64), CD16/32 (FCγ III/II receptor, clone 2.4G2), and Fixable viability dye (ef780, Zombie NIR)

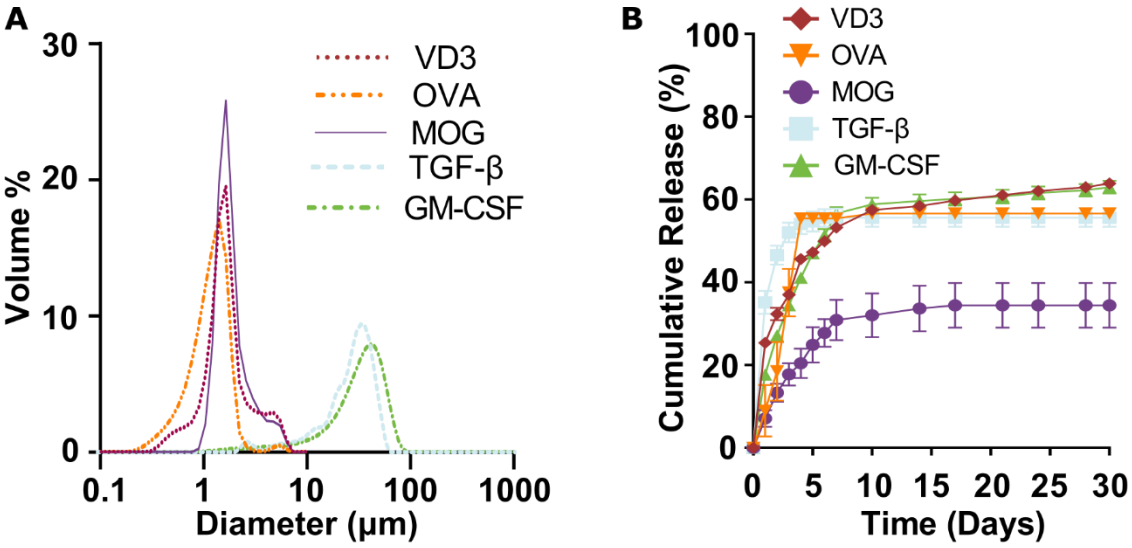

C

Agent	Diameter ± SD (µm)	Polydispersity Index	Mass Loaded (µg)/ 500 mg of PLGA	Encapsulation Efficiency ± SD (%)	Mass Injected ± SD (ng)
Vitamin D_3	1.6 ± 0.93	0.34	50	76 ± 1.6	190 ± 4
OVA	0.80 ± 0.41	0.26	4000	48 ± 7.1	9600 ± 1428
MOG	2.5 ± 1.2	0.23	4000	38 ± 3.5	7694 ± 698
TGF-β	30 ± 13	0.19	25	44 ± 9.3	55 ± 12
GM-CSF	36 ± 18	0.25	40	69 ± 7.8	139 ± 16

Figure S1. dMP characterization a) Size quantification of MPs by dynamic light scattering. b) Release kinetics of each agent encapsulated measured over 30 days. c) Sizing, polydispersity index, loading amount, encapsulation efficiency, and dose per injection for MPs containing each agent. Polydispersity index was calculated as standard deviation divided by mean diameter quantity squared.

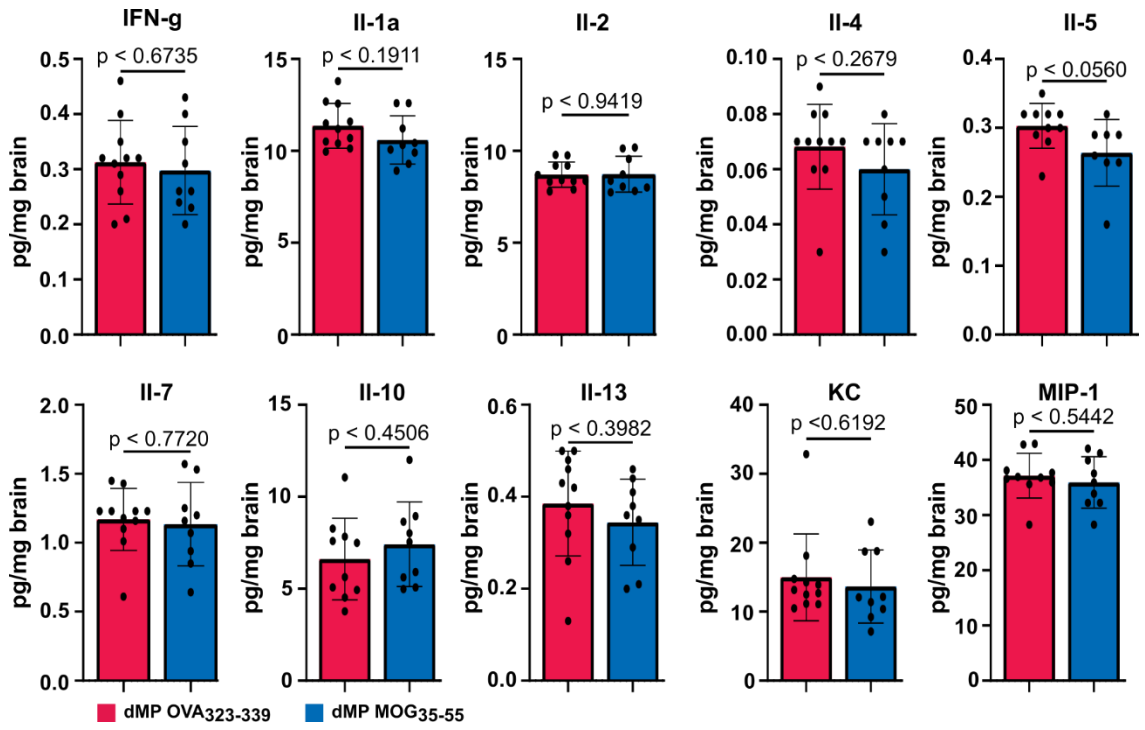

Fig. S2. Cytokines less correlated with MS were not differently produced in the CNS between dMP MOG vs. dMP OVA treatment. Luminex xMAP technology multiplexed quantification of Mouse cytokines, chemokines, and growth factors from complete brain homogenate at a concentration of 4 mg/mL on day 7 post treatment. n=8-11 * represents $p < 0.05$, ** represents $p < 0.01$

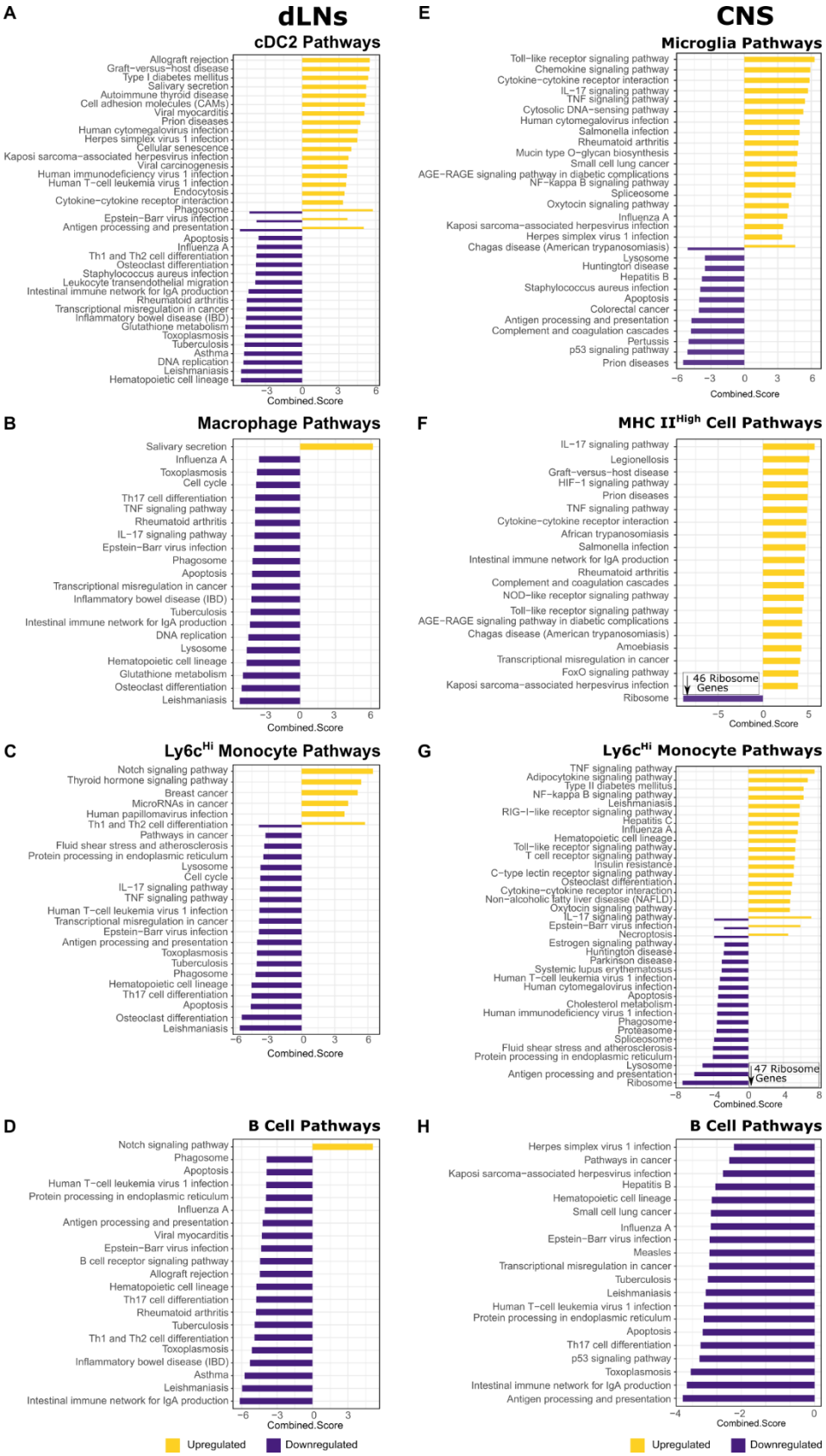
A
dLNs
cDC2 Pathways
Allograft rejection
Graft−versus−host disease
Type I diabetes mellitus
Salivary secretion
Autoimmune thyroid disease
Cell adhesion molecules (CAMs)
Viral myocarditis
Prion diseases
Human cytomegalovirus infection
Herpes simplex virus 1 infection
Cellular senescence
Kaposi sarcoma−associated herpesvirus infection
Viral carcinogenesis
Human immunodeficiency virus 1 infection
Human T−cell leukemia virus 1 infection
Endocytosis
Cytokine−cytokine receptor interaction
Phagosome
Epstein−Barr virus infection
Antigen processing and presentation
Apoptosis
Influenza A
Th1 and Th2 cell differentiation
Osteoclast differentiation
Staphylococcus aureus infection
Leukocyte transendothelial migration
Intestinal immune network for IgA production
Rheumatoid arthritis
Transcriptional misregulation in cancer
Inflammatory bowel disease (IBD)
Glutathione metabolism
Toxoplasmosis
Tuberculosis
Asthma
DNA replication
Leishmaniasis
Hematopoietic cell lineage
−3 0 3 6
Combined.Score
B
Macrophage Pathways
Salivary secretion
Influenza A
Toxoplasmosis
Cell cycle
Th17 cell differentiation
TNF signaling pathway
Rheumatoid arthritis
IL−17 signaling pathway
Epstein−Barr virus infection
Phagosome
Apoptosis
Transcriptional misregulation in cancer
Inflammatory bowel disease (IBD)
Tuberculosis
Intestinal immune network for IgA production
DNA replication
Lysosome
Hematopoietic cell lineage
Glutathione metabolism
Osteoclast differentiation
Leishmaniasis
−3 0 3 6
Combined.Score
C
Ly6c^Hi Monocyte Pathways
Notch signaling pathway
Thyroid hormone signaling pathway
Breast cancer
MicroRNAs in cancer
Human papillomavirus infection
Th1 and Th2 cell differentiation
Pathways in cancer
Fluid shear stress and atherosclerosis
Protein processing in endoplasmic reticulum
Lysosome
Cell cycle
IL−17 signaling pathway
TNF signaling pathway
Human T−cell leukemia virus 1 infection
Transcriptional misregulation in cancer
Epstein−Barr virus infection
Antigen processing and presentation
Toxoplasmosis
Tuberculosis
Phagosome
Hematopoietic cell lineage
Th17 cell differentiation
Apoptosis
Osteoclast differentiation
Leishmaniasis
−6 −3 0 3 6
Combined.Score
D
B Cell Pathways
Notch signaling pathway
Phagosome
Apoptosis
Human T−cell leukemia virus 1 infection
Protein processing in endoplasmic reticulum
Influenza A
Antigen processing and presentation
Viral myocarditis
Epstein−Barr virus infection
B cell receptor signaling pathway
Allograft rejection
Hematopoietic cell lineage
Th17 cell differentiation
Rheumatoid arthritis
Tuberculosis
Th1 and Th2 cell differentiation
Toxoplasmosis
Inflammatory bowel disease (IBD)
Asthma
Leishmaniasis
Intestinal immune network for IgA production
−6 −3 0 3
Combined.Score
Upregulated
Downregulated
E
CNS
Microglia Pathways
Toll−like receptor signaling pathway
Chemokine signaling pathway
Cytokine−cytokine receptor interaction
IL−17 signaling pathway
TNF signaling pathway
Cytosolic DNA−sensing pathway
Human cytomegalovirus infection
Salmonella infection
Rheumatoid arthritis
Mucin type O−glycan biosynthesis
Small cell lung cancer
AGE−RAGE signaling pathway in diabetic complications
NF−kappa B signaling pathway
Spliceosome
Oxytocin signaling pathway
Influenza A
Kaposi sarcoma−associated herpesvirus infection
Herpes simplex virus 1 infection
Chagas disease (American trypanosomiasis)
Lysosome
Huntington disease
Hepatitis B
Staphylococcus aureus infection
Apoptosis
Colorectal cancer
Antigen processing and presentation
Complement and coagulation cascades
Pertussis
p53 signaling pathway
Prion diseases
−6 −3 0 3 6
Combined.Score
F
MHC II^High Cell Pathways
IL−17 signaling pathway
Legionellosis
Graft−versus−host disease
HIF−1 signaling pathway
Prion diseases
TNF signaling pathway
Cytokine−cytokine receptor interaction
African trypanosomiasis
Salmonella infection
Intestinal immune network for IgA production
Rheumatoid arthritis
Complement and coagulation cascades
NOD−like receptor signaling pathway
Toll−like receptor signaling pathway
AGE−RAGE signaling pathway in diabetic complications
Chagas disease (American trypanosomiasis)
Amoebiasis
Transcriptional misregulation in cancer
FoxO signaling pathway
Kaposi sarcoma−associated herpesvirus infection
Ribosome
46 Ribosome Genes
−5 0 5
Combined.Score
G
Ly6c^Hi Monocyte Pathways
TNF signaling pathway
Adipocytokine signaling pathway
Type II diabetes mellitus
NF−kappa B signaling pathway
Leishmaniasis
RIG−I−like receptor signaling pathway
Hepatitis C
Influenza A
Hematopoietic cell lineage
Toll−like receptor signaling pathway
T cell receptor signaling pathway
Insulin resistance
C−type lectin receptor signaling pathway
Osteoclast differentiation
Cytokine−cytokine receptor interaction
Non−alcoholic fatty liver disease (NAFLD)
Oxytocin signaling pathway
IL−17 signaling pathway
Epstein−Barr virus infection
Necroptosis
Estrogen signaling pathway
Huntington disease
Parkinson disease
Systemic lupus erythematosus
Human T−cell leukemia virus 1 infection
Human cytomegalovirus infection
Apoptosis
Cholesterol metabolism
Human immunodeficiency virus 1 infection
Phagosome
Proteasome
Spliceosome
Fluid shear stress and atherosclerosis
Protein processing in endoplasmic reticulum
Lysosome
Antigen processing and presentation
Ribosome
47 Ribosome Genes
−8 −4 0 4 8
Combined.Score
H
B Cell Pathways
Herpes simplex virus 1 infection
Pathways in cancer
Kaposi sarcoma−associated herpesvirus infection
Hepatitis B
Hematopoietic cell lineage
Small cell lung cancer
Influenza A
Epstein−Barr virus infection
Measles
Transcriptional misregulation in cancer
Tuberculosis
Leishmaniasis
Human T−cell leukemia virus 1 infection
Protein processing in endoplasmic reticulum
Apoptosis
Th17 cell differentiation
p53 signaling pathway
Toxoplasmosis
Intestinal immune network for IgA production
Antigen processing and presentation
−4 −2 0
Combined.Score
Upregulated
Downregulated

Fig. S3. APCs downregulated Antigen presentation, activation and Pro-inflammatory pathway genes in both the dLNs and CNS. Pathways modulated in a) cDC2s, b) macrophages, c) Ly6c^{Hi} monocytes and d) B cells located in the dLNs at day 2, specifically antigen presentation. Pathways modulated in e) microglia, f) MHC II^{High} cells, g) Ly6c^{Hi} monocytes and h) B cells in the spinal cord at day 7, specifically antigen presentation and ribosome. Genes with $p_{adjusted}$ <0.1 were used in pathway analysis. Significant genes were compared to the KEGG pathways and $p_{adjusted}$ <0.1 denoted a pathway was up or downregulated. n=2 mice per group in the dLNs and n=1 mouse per group in the CNS

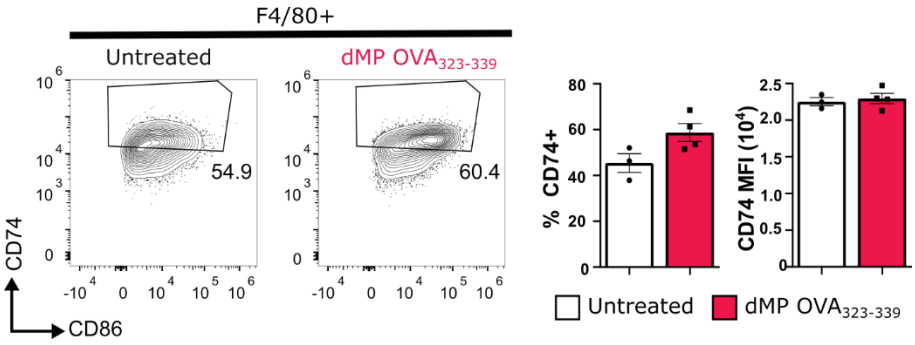

Figure S4. dMP OVA treatment in mice with advanced EAE does not results in reduction in MHCII components in macrophages. Representative flow plots and quantification of CD74 in the spinal cord on day 7 in macrophages.

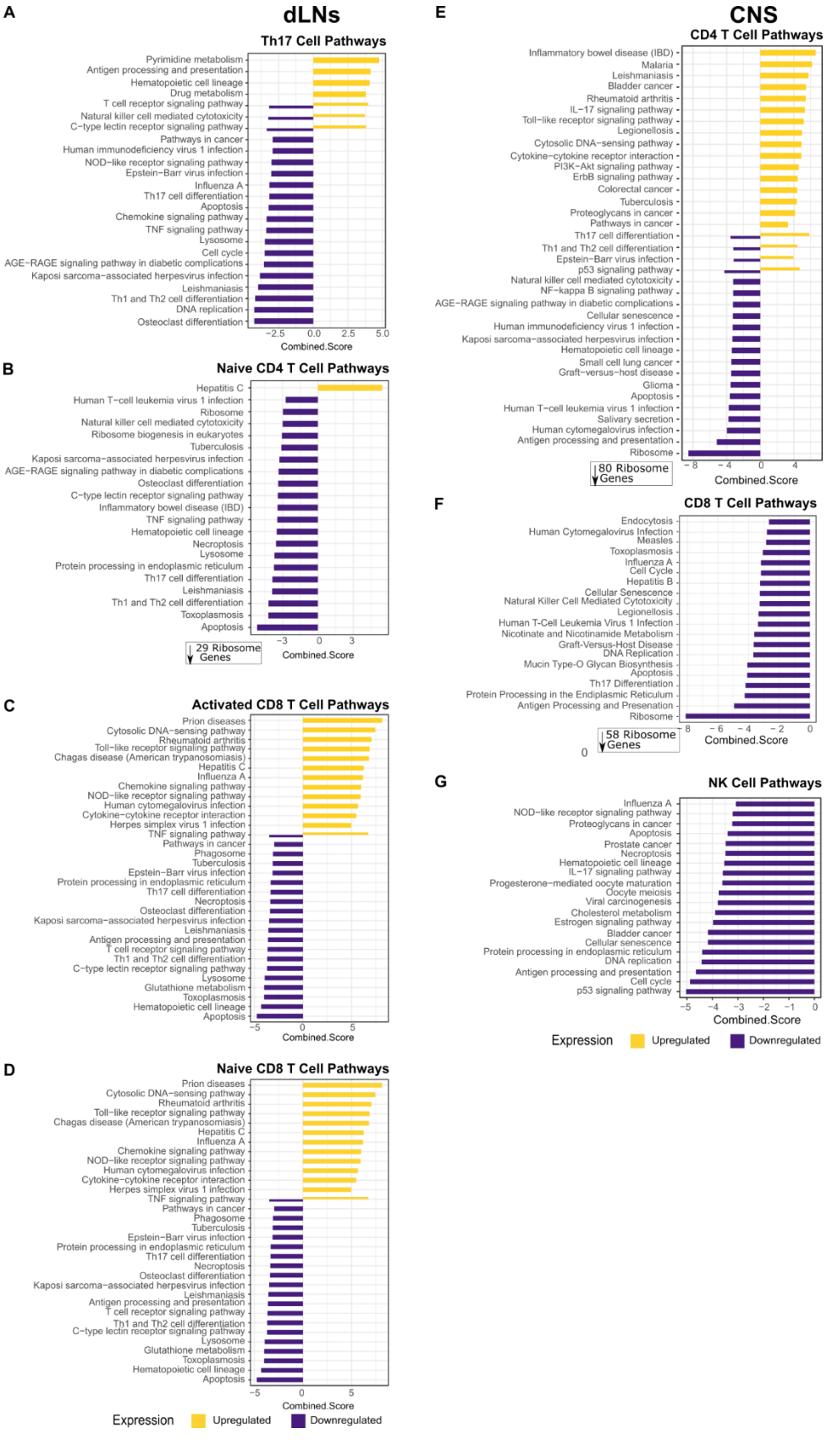
A
dLNs
Th17 Cell Pathways
Pyrimidine metabolism
Antigen processing and presentation
Hematopoietic cell lineage
Drug metabolism
T cell receptor signaling pathway
Natural killer cell mediated cytotoxicity
C−type lectin receptor signaling pathway
Pathways in cancer
Human immunodeficiency virus 1 infection
NOD−like receptor signaling pathway
Epstein−Barr virus infection
Influenza A
Th17 cell differentiation
Apoptosis
Chemokine signaling pathway
TNF signaling pathway
Lysosome
Cell cycle
AGE−RAGE signaling pathway in diabetic complications
Kaposi sarcoma−associated herpesvirus infection
Leishmaniasis
Th1 and Th2 cell differentiation
DNA replication
Osteoclast differentiation
−2.5
0.0
2.5
5.0
Combined.Score
B
Naive CD4 T Cell Pathways
Hepatitis C
Human T−cell leukemia virus 1 infection
Ribosome
Natural killer cell mediated cytotoxicity
Ribosome biogenesis in eukaryotes
Tuberculosis
Kaposi sarcoma−associated herpesvirus infection
AGE−RAGE signaling pathway in diabetic complications
Osteoclast differentiation
C−type lectin receptor signaling pathway
Inflammatory bowel disease (IBD)
TNF signaling pathway
Hematopoietic cell lineage
Necroptosis
Lysosome
Protein processing in endoplasmic reticulum
Th17 cell differentiation
Leishmaniasis
Th1 and Th2 cell differentiation
Toxoplasmosis
Apoptosis
29 Ribosome Genes
−3
0
3
Combined.Score
C
Activated CD8 T Cell Pathways
Prion diseases
Cytosolic DNA−sensing pathway
Rheumatoid arthritis
Toll−like receptor signaling pathway
Chagas disease (American trypanosomiasis)
Hepatitis C
Influenza A
Chemokine signaling pathway
NOD−like receptor signaling pathway
Human cytomegalovirus infection
Cytokine−cytokine receptor interaction
Herpes simplex virus 1 infection
TNF signaling pathway
Pathways in cancer
Phagosome
Tuberculosis
Epstein−Barr virus infection
Protein processing in endoplasmic reticulum
Th17 cell differentiation
Necroptosis
Osteoclast differentiation
Kaposi sarcoma−associated herpesvirus infection
Leishmaniasis
Antigen processing and presentation
T cell receptor signaling pathway
Th1 and Th2 cell differentiation
C−type lectin receptor signaling pathway
Lysosome
Glutathione metabolism
Toxoplasmosis
Hematopoietic cell lineage
Apoptosis
−5
0
5
Combined.Score
D
Naive CD8 T Cell Pathways
Prion diseases
Cytosolic DNA−sensing pathway
Rheumatoid arthritis
Toll−like receptor signaling pathway
Chagas disease (American trypanosomiasis)
Hepatitis C
Influenza A
Chemokine signaling pathway
NOD−like receptor signaling pathway
Human cytomegalovirus infection
Cytokine−cytokine receptor interaction
Herpes simplex virus 1 infection
TNF signaling pathway
Pathways in cancer
Phagosome
Tuberculosis
Epstein−Barr virus infection
Protein processing in endoplasmic reticulum
Th17 cell differentiation
Necroptosis
Osteoclast differentiation
Kaposi sarcoma−associated herpesvirus infection
Leishmaniasis
Antigen processing and presentation
T cell receptor signaling pathway
Th1 and Th2 cell differentiation
C−type lectin receptor signaling pathway
Lysosome
Glutathione metabolism
Toxoplasmosis
Hematopoietic cell lineage
Apoptosis
−5
0
5
Combined.Score
Expression
Upregulated
Downregulated
E
CNS
CD4 T Cell Pathways
Inflammatory bowel disease (IBD)
Malaria
Leishmaniasis
Bladder cancer
Rheumatoid arthritis
IL−17 signaling pathway
Toll−like receptor signaling pathway
Legionellosis
Cytosolic DNA−sensing pathway
Cytokine−cytokine receptor interaction
PI3K−Akt signaling pathway
ErbB signaling pathway
Colorectal cancer
Tuberculosis
Proteoglycans in cancer
Pathways in cancer
Th17 cell differentiation
Th1 and Th2 cell differentiation
Epstein−Barr virus infection
p53 signaling pathway
Natural killer cell mediated cytotoxicity
NF−kappa B signaling pathway
AGE−RAGE signaling pathway in diabetic complications
Cellular senescence
Human immunodeficiency virus 1 infection
Kaposi sarcoma−associated herpesvirus infection
Hematopoietic cell lineage
Small cell lung cancer
Graft−versus−host disease
Glioma
Apoptosis
Human T−cell leukemia virus 1 infection
Salivary secretion
Human cytomegalovirus infection
Antigen processing and presentation
Ribosome
80 Ribosome Genes
−8
−4
0
4
Combined.Score
F
CD8 T Cell Pathways
Endocytosis
Human Cytomegalovirus Infection
Measles
Toxoplasmosis
Influenza A
Cell Cycle
Hepatitis B
Cellular Senescence
Natural Killer Cell Mediated Cytotoxicity
Legionellosis
Human T-Cell Leukemia Virus 1 Infection
Nicotinate and Nicotinamide Metabolism
Graft-Versus-Host Disease
DNA Replication
Mucin Type-O Glycan Biosynthesis
Apoptosis
Th17 Differentiation
Protein Processing in the Endiplasmic Reticulum
Antigen Processing and Presenation
Ribosome
58 Ribosome Genes
0
−8
−6
−4
−2
0
Combined.Score
G
NK Cell Pathways
Influenza A
NOD−like receptor signaling pathway
Proteoglycans in cancer
Apoptosis
Prostate cancer
Necroptosis
Hematopoietic cell lineage
IL−17 signaling pathway
Progesterone−mediated oocyte maturation
Oocyte meiosis
Viral carcinogenesis
Cholesterol metabolism
Estrogen signaling pathway
Bladder cancer
Cellular senescence
Protein processing in endoplasmic reticulum
DNA replication
Antigen processing and presentation
Cell cycle
p53 signaling pathway
−5
−4
−3
−2
−1
0
Combined.Score
Expression
Upregulated
Downregulated

Fig. S5. T Cells downregulated Pro-inflammatory and activation pathways in both the dLNs and CNS. Pathways modulated in a) Th17 Cells, b) naïve CD4+ T cells, c) Activated CD8+ T cells and d) naïve CD8+ T cells located in the dLNs at day 2, including ribosome and DNA replication. Pathways modulated in e) CD4+ T cells, f) CD8+ T cells and g) NK cells in the spinal cord at day 7. Genes with padjusted <0.1 were used in pathway analysis. Significant genes were compared to the KEGG pathways and padjusted <0.1 denoted a pathway was up or downregulated. n=2 mice per group in the dLNs and n=1 mouse per group in the CNS.

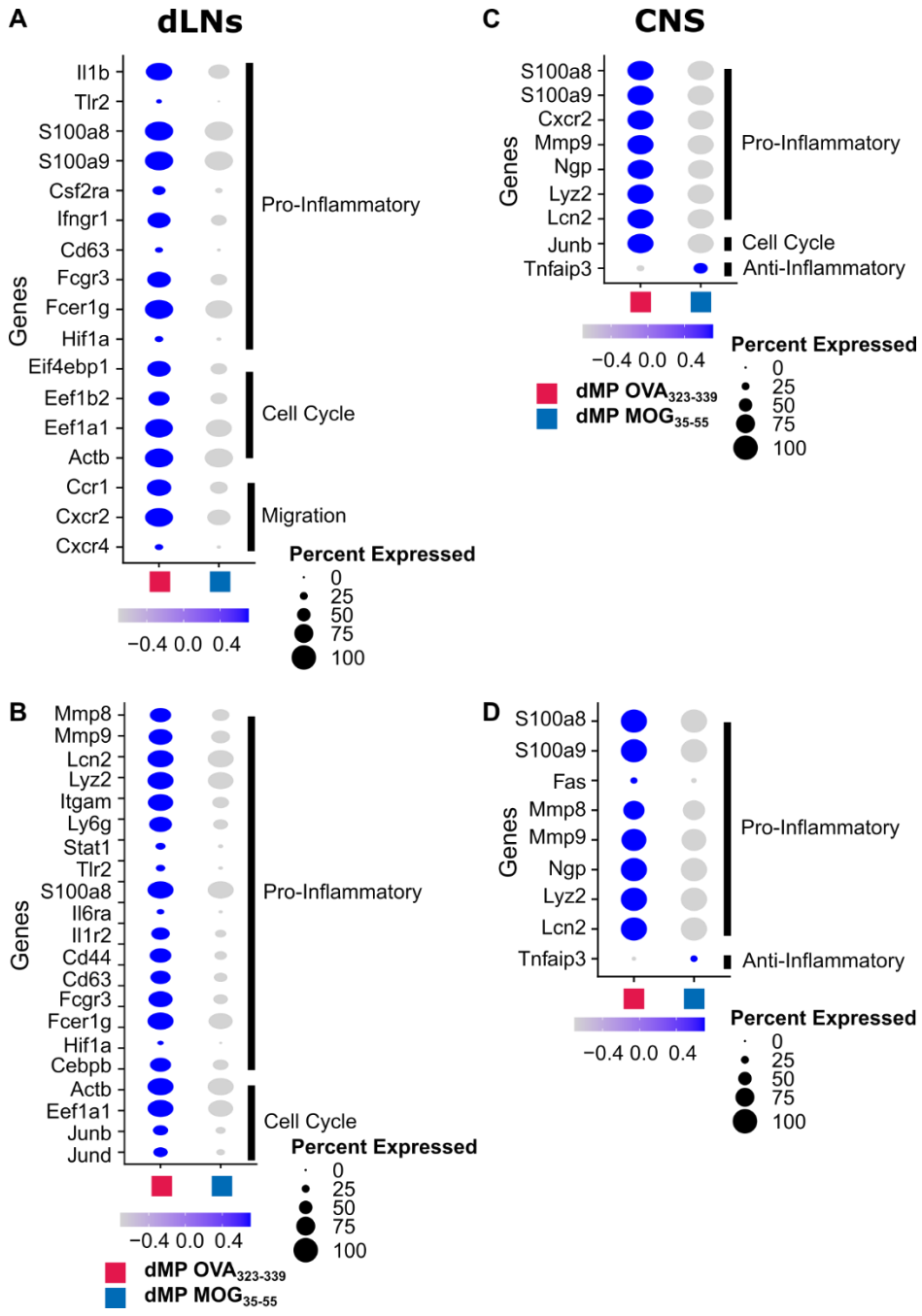

Fig. S6. Neutrophils downregulate pro-inflammatory and cell cycle genes in the dLNs and CNS. Dot plots highlighting pro-inflammatory, cell cycle, and migration genes differentially expressed in a) inflammatory neutrophils and b) suppressive neutrophils, specifically genes associated with pro-inflammatory processes in the dLNs at day 2. Dot

plots showing downregulation of pro-inflammatory and upregulation of anti-inflammatory genes in the c) inflammatory and d) suppressive neutrophils located in the CNS at day 7. Genes with a $p_{adjusted}$ <0.1 of were considered significant. n=2 mice per group in the dLNs and n=1 mouse per group in the CNS**.**

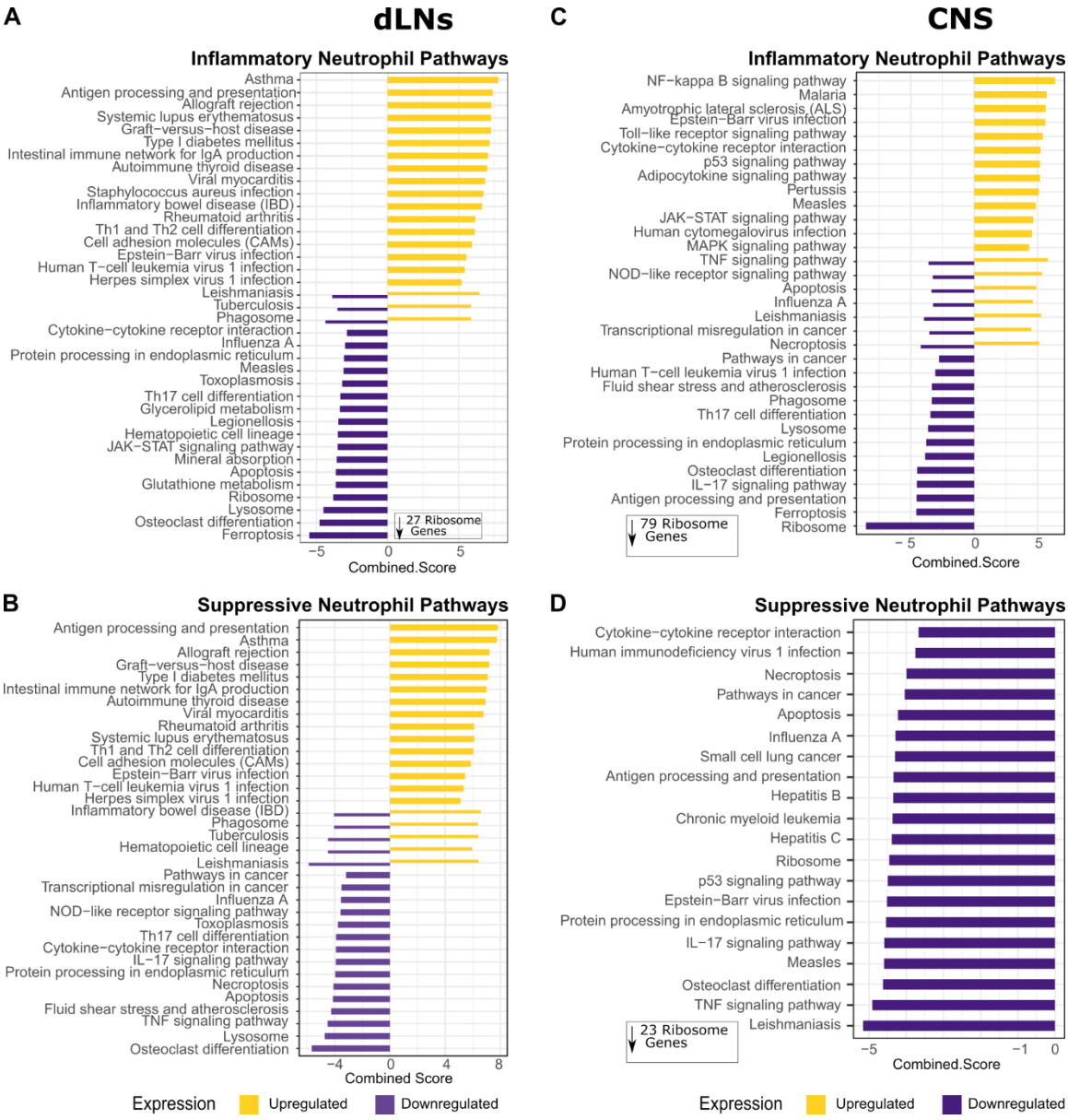

Fig. S7. Neutrophils downregulated Pro-inflammatory pathways in both the dLNs and CNS. Pathways modulated in a) inflammatory neutrophils and b) Suppressive neutrophils located in the dLNs at day 2, including ribosome and phagocytosis. Pathways modulated in c) inflammatory neutrophils and d) Suppressive neutrophils located in the CNS at day 7, including ribosome. Genes with $p_{adjusted}$ <0.1 were used in pathway analysis. Significant genes were compared to the KEGG pathways and $p_{adjusted}$

<0.1 denoted a pathway was up or downregulated. n=2 mice per group in the dLNs and n=1 mouse per group in the CNS.